

RESEARCH

Open Access



Extracellular vesicles isolated from adipose tissue-derived mesenchymal stromal cells as carriers for Paclitaxel delivery

Angela Marcianti¹ , Eleonora Spampinato¹ , Sara Nava¹ , Giulia Maria Stella^{2,3} , Paola Perego⁴ ,
Simona Pogliani¹ , Simona Frigerio¹ , Luca Mirra⁴ , Paola Gagni⁵ , Fabio Moda^{6,7} ,
Federico Angelo Cazzaniga⁷ , Giovanni Luca Beretta⁴ , Guido Maronati⁸, Giuseppe Paglia⁹ ,
Angelo Guido Corsico^{2,3} , Catia Traversari¹ and Daniela Lisini^{1*}

Abstract

Background Mesenchymal Stromal Cells (MSC)-derived Extracellular Vesicles (EV) represent innovative tools for drug delivery systems. However, their clinical use is limited by the lack of standardized good manufacturing practice (GMP)-compliant isolation and conservation protocols. In this study, we developed a GMP-compliant protocol for the preparation of MSC-EVs and investigated the feasibility of producing EVs loaded with paclitaxel (PTX) for clinical application as drug products.

Methods Adipose tissues from 13 donors were used to obtain MSC-EVs via culture supernatant ultracentrifugation. EVs loaded with PTX were manufactured by adding the drug to the culture medium of MSCs before supernatant collection. EV identity was verified in terms of concentration/size, protein content, morphology, and expression of EV surface markers. The anti-proliferative activity, accumulation ability in tumor cells and PTX content, as well as their stability over time, were also evaluated.

Results High numbers of EV/EV-PTX compliant in terms of integrity/identity were obtained and can be successfully stored for up to one year at -80 °C. Cellular studies have shown that EVs are capable of accumulating in tumor cells and, when loaded with PTX, inhibiting the proliferation of a pleural mesothelioma cell line.

Conclusions These results support the potential future clinical use of EVs as carriers for drug delivery to improve cancer treatment strategies.

Keywords Extracellular vesicles, Mesenchymal stromal cells, Paclitaxel, Antitumor drug, Drug delivery systems

*Correspondence:

Daniela Lisini

daniela.lisini@istituto-besta.it

¹Cell Therapy Production Unit, Scientific Direction, IRCCS Neurologic Institute C. Besta Foundation, 20133 Milan, Italy

²Department of Internal Medicine and Medical Therapeutics, University of Pavia Medical School, Pavia, Italy

³Cardiothoracic and Vascular Department, Unit of Respiratory Diseases, IRCCS San Matteo Hospital Foundation, Pavia, Italy

⁴Molecular Pharmacology Unit, Fondazione IRCCS Istituto Nazionale dei Tumori, Milan, Italy

⁵Istituto di Scienze e Tecnologie Chimiche “Giulio Natta”, National Research Council of Italy (SCITEC-CNR), 20131 Milan, Italy

⁶Department of Medical Biotechnology and Translational Medicine, University of Milan, Milan, Italy

⁷Unit of Laboratory Medicine, Laboratory of Clinical Pathology, IRCCS Neurologic Institute C. Besta Foundation, Milan, Italy

⁸Synlab CAM Polidiagnostico, 20900 Monza, Italy

⁹School of Medicine and Surgery, Milano-Bicocca University, 20900 Monza, Italy



© The Author(s) 2025. **Open Access** This article is licensed under a Creative Commons Attribution-NonCommercial-NoDerivatives 4.0 International License, which permits any non-commercial use, sharing, distribution and reproduction in any medium or format, as long as you give appropriate credit to the original author(s) and the source, provide a link to the Creative Commons licence, and indicate if you modified the licensed material. You do not have permission under this licence to share adapted material derived from this article or parts of it. The images or other third party material in this article are included in the article's Creative Commons licence, unless indicated otherwise in a credit line to the material. If material is not included in the article's Creative Commons licence and your intended use is not permitted by statutory regulation or exceeds the permitted use, you will need to obtain permission directly from the copyright holder. To view a copy of this licence, visit <http://creativecommons.org/licenses/by-nc-nd/4.0/>.

Introduction

In recent years, Extracellular Vesicles (EV) have emerged as promising and innovative tools for drug delivery, offering a wide range of potential applications that could revolutionize patient care and outcomes.

EVs are small particles that are delimited by a lipid bilayer and carry a cargo of proteins, nucleic acids and lipids but cannot replicate on their own. Recent studies have highlighted the potential benefits of Mesenchymal Stromal Cell-derived EVs (MSC-EVs), which have been shown to maintain the same therapeutic effects as MSCs without potential disadvantages, such as the risk of tumor formation [1, 2]. Compared with the majority of the biological effect EVs derived from other cell types, MSC-EVs are characterized by higher stability, lower immunogenicity, and the possibility of being engineered to display therapeutic effects [3]. Indeed, the high potential of MSC-EVs as Drug Delivery System (DDS) to treat different diseases has been described, as the lipid bilayer membrane of EVs can support both hydrophilic and hydrophobic drugs [4, 5]. EVs can cross the blood–brain barrier, a feature that makes them especially interesting as natural carriers of drugs for curing neurodegenerative diseases [6]. MSC-EVs are also used as DDS in cardiovascular, nervous, kidney and skin diseases, with the primary aim of strongly improving treatment efficacy and limiting systemic adverse events [7–12].

The characteristics of MSC-EVs make them suitable candidates for use as DDSs in neoplastic diseases due to various possible advantages: (i) the delivered drugs could be better localized to the tumor site, reducing the interaction between the drug and normal cells, thereby contributing to limit systemic toxicity; (ii) the drug concentration in the tumor environment could be enhanced, increasing tumor drug uptake and, again, reducing side effects; (iii) pharmacological therapy could be carried out using a reduced amount of drug, compared with the conventional dose; and (iv) the bioavailability of the drugs already used in standard therapy could be increased via new routes of administration [13–16]. Moreover, since EVs cannot replicate, the safety of EV-based approaches is greater than that of cell-based therapies.

Although the approval of MSC-EVs as drug product from regulatory agencies could be facilitated for all these reasons, the clinical use of EVs is limited to date by the lack of robust and standardized good manufacturing practice (GMP)-compliant preparation and conservation protocols.

MSC-EV preparation is a complex process that involves many critical steps, starting from the choice of the cell source to the MSC isolation methods and the culture conditions. Indeed, compliance of the primary cells is considered mandatory to obtain an EV product of acceptable quality. The choice of culture medium is also

a critical issue, as although medium supplemented with platelet lysate represents the best choice of many laboratories to improve the MSC growth rate, the use of platelet lysate can lead to impurities in the final product (i.e., EVs of plasma origin). Among the critical steps, the EV isolation method and the choice of phenotypic and functional EV characterization methods are crucial as well. It has been widely demonstrated that different sources and protocols lead to different products in terms of identity, quantity and efficacy [17–19]. Moreover, there is limited knowledge about the optimal storage conditions or time, shelf life and stability, all of which are key points for the use of EVs as medicinal products.

Since 2010, our laboratory has focused on the development and manufacturing of cell therapy medicinal products and is now involved in the manufacturing and quality control of MSCs loaded with Paclitaxel (PTX) used as a drug product to treat patients with mesothelioma enrolled in a new clinical trial (PacliMES), approved by ISS and AIFA [20].

The aims of the present study were to explore the possibility of (a) setting up a GMP-compliant protocol for the preparation of MSC-EVs, starting from lipoaspirated Adipose Tissue (AT) from healthy donors, for use in therapeutic approaches and (b) preparing EVs loaded with PTX for potential clinical application as antitumor drug products.

Materials and methods

Sample collection

AT lipoaspirates were collected under general anesthesia from 13 healthy volunteer donors (9/13 females and 4/13 males) undergoing plastic surgery for aesthetic purposes. The mean age was 46.4 years (range: 20–63 years). Samples were collected after signed informed consent was obtained for the use of surgical tissues (otherwise destined for destruction) in accordance with the Declaration of Helsinki. Informed consent was obtained prior to tissue collection, and the Institutional Review Board of the IRCCS Neurological Institute C. Besta Foundation approved the design of the study (n. 15, 29/03/23).

The AT samples were processed within 24 h from surgery.

MSC isolation and expansion and supernatants collection

MSCs from AT lipoaspirates were isolated and expanded as described previously [21]– [22]. Briefly, samples were disaggregated by enzymatic digestion with 0.3 PZU of collagenase type I (Life Technologies, USA) and then centrifuged (300xg, 15 min), and the floating fraction and cellular pellet were plated in 150 cm² flasks (Euroclone, UK), 10 mL/flask in DMEM (Euroclone, UK) supplemented with 5% platelet lysate and 2 mM L-glutamine (Euroclone, UK). MultiPL100 (Macopharma, France)

and Stemulate (Sextonbio, USA), both derived from platelets of more than 100 donors, were used as platelet lysates. The flasks were maintained at 37 °C in a humidified atmosphere containing 5% CO₂ and checked twice weekly; medium was added (2 mL) every 3–4 days. When the MSC sprouted from the lipoaspirated AT, the tissue, detached from the plastic support, is collected together with the culture medium. Cells were washed twice with 5 ml of PBS and new culture medium was added to the flasks (10 ml/flask). After reaching 80% confluence, the MSCs were harvested via TrypLe solution (Sigma-Aldrich, USA) and propagated at 4,000 cells/cm² until the passage did not exceed passage 4 (P4).

Twenty-four hours before supernatant collection, the complete medium of MSC cultures not exceeding 50–60% confluence was replaced with medium without platelet lysate (starvation) to deprive supernatants from EVs of lysate origin and to stimulate the maximum EV release from cells. After 24 h, the supernatants were collected and processed immediately or cryopreserved at -80 °C.

MSCs were detached and characterized in terms of morphology, number and viability, Population Doubling Time (PDT), and the expression of the typical MSC markers CD90, CD73, and CD105 and the hematopoietic/endothelial markers CD34, CD45 and CD31, as described previously [21].

Drug loading of MSCs with PTX and supernatants collection

To obtain MSC-EVs loaded with PTX (EV-PTX), cells at a maximum confluence of 50–60% were treated with PTX (final concentration 10 µg/mL; PTX, TEVA, IT, 6 mg/mL) for 20–22 h before supernatant collection. For this purpose, complete medium without PTX was rapidly replaced with complete medium supplemented with PTX. After 20–22 h of incubation at 37 °C and 5% CO₂, the complete medium containing PTX was replaced with basal DMEM alone. The supernatants were collected 24 h after replacement.

EV and EV-PTX isolation and storage

EV were isolated immediately or after the cryoconservation of the culture supernatant (SUP), supplemented or not with 1% Dimethyl Sulfoxide (Cryosure DMSO GMP grade, Li StarFISH) at -80 °C, to test the possibility of cryoconservation of the supernatants. EV-PTX were isolated immediately after SUP collection. EV were purified starting from 80 ml supernatant in each experiment. EV and EV-PTX isolation was performed by ultracentrifugation. Briefly, SUP were centrifuged first at 800xg for 20 min at 4 °C to eliminate debris and dead cells and then at 100000xg for 1 h at 4 °C. EVs were cryopreserved in

sterile solutions of 0.9% NaCl (pharmaceutical grade) supplemented or not of 1% DMSO at -80 °C.

Assessment of EV and EV-PTX identity

Nanoparticle tracking analysis (NTA)

The concentration and size distribution of EV and EV-PTX were assessed using the NanoSight NS300 system (Malvern Technologies, Malvern, UK) configured with a 532 nm laser and NTA software version 3.4 to perform Nanoparticle Tracking Analysis (NTA), according to the manufacturer's instructions. Settings were adjusted as follows: a syringe pump with constant flow injection was used, and three videos of 60 s each were captured to obtain the mean concentrations expressed as particles/mL and mode size. The samples were diluted with filtered Phosphate Buffer Salt (PBS) to a final volume of 1 mL to yield the ideal particle per frame value, ranging from 20 to 100 particles/frame, which corresponds to a particle concentration in the range of 1×10^7 to 1×10^9 particles/mL.

Measurement of total protein content

A micro BCA protein assay kit (Thermo Fisher Scientific, USA) was used to determine the total protein concentration. The samples were lysed with RIPA buffer (1:1) for 30 min on ice before the test was performed. The assay was carried out following the manufacturer's instructions. The absorbance values were read in a Victor NIVO (Perkin Elmer, USA) at a wavelength of 562 nm, and the protein concentrations of the samples were quantified using a standard curve.

Transmission electron microscopy (TEM)

Ten microliters of isolated EV and EV-PTX were carefully deposited onto 200-mesh Formvar-carbon coated nickel grids and incubated for 30 min. After incubation, the excess solution was blotted dry using filter paper. The grids were then subjected to negative staining with 25% Uranyl Acetate Replacement (UAR) for 10 min. Following the staining, the UAR solution was removed with filter paper, and the grids were air-dried for 20 min prior to analysis. Imaging was performed at 120 kV using a FEI Tecnai Spirit transmission electron microscope, equipped with an Olympus Megaview G2 camera.

Flow cytometry analysis of surface markers

EV and EV-PTX surface markers were evaluated by flow cytometry using the MACSplex Exosome Kit (Miltenyi Biotec, Bergisch Gladbach, Germany), analyzing 37 surface markers simultaneously, following the manufacturer's instructions and as described by Las Heras et al. [23]. The 37 surface markers are detailed in Table 1.

Briefly, 1×10^9 EV/EV-PTX were diluted to 120 µL with MACSplex buffer and incubated for 15 min at Room

Table 1 Surface marker antibodies used in the macsplex exosome kit

Antibody	Isotype	Antibody	Isotype
CD3	Mouse IgG2a	CD81	Recombinant human IgG1
CD4	Mouse IgG2a	MCSP	Mouse IgG1
CD19	Mouse IgG1	CD146	Mouse IgG1
CD8	Mouse IgG2a	CD41b	Recombinant human IgG1
HLA-DRDPDQ	Recombinant human IgG1	CD42a	Recombinant human IgG1
CD56	Recombinant human IgG1	CD24	Mouse IgG1
CD105	Recombinant human IgG1	CD86	Mouse IgG1
CD2	Mouse IgG2b	CD44	Mouse IgG1
CD1c	Mouse IgG2a	CD326	Mouse IgG1
CD25	Mouse IgG1	CD133/1	Mouse IgG1k
CD49e	Recombinant human IgG1	CD29	Mouse IgG1k
ROR1	Mouse IgG1k	CD69	Mouse IgG1k
CD209	Mouse IgG1	CD142	Mouse IgG1k
CD9	Mouse IgG1	CD45	Mouse IgG2a
SSEA-4	Recombinant human IgG1	CD31	Mouse IgG1
HLA-ABC	Recombinant human IgG1	REA Control	Recombinant human IgG1
CD63	Mouse IgG1k	CD20	Mouse IgG1
CD40	Mouse IgG1k	CD14	Mouse IgG2a
CD62p	Recombinant human IgG1	mlgG1 Control	Mouse IgG1
CD11c	Mouse IgG2b		

Overview of the surface marker antibodies used in the MACSPlex Exosome Kit. CD: cluster of differentiation

Temperature (RT) in a 1.5 mL tube. Then, 15 µL of EV capture beads and 15 µL of EV detection reagent mixture (CD9, CD63 and CD81) were added to each tube and incubated for 1 h at RT under agitation. For the blank control, only MACSPlex buffer was used. Next, 500 µL of MACSPlex buffer was added to each tube, and the tubes were centrifuged at 3000xg for 5 min at RT. The samples were subsequently washed with 500 µL of MACSPlex buffer and centrifuged again. After the supernatants were removed, the samples were resuspended in MACSPlex buffer and transferred to a flow cytometry tube. Samples were acquired using the MACSQuant flow cytometer (Miltenyi Biotec, Bergisch Gladbach, Germany) and the data were analyzed with the MACSQuant analyzer 10 Software (Miltenyi Biotec, Bergisch Gladbach, Germany). The 37 single bead populations were gated to determine the APC signal intensity on each bead population and the Median Fluorescence Intensity (MFI) for each capture bead was measured. For each population, the background was corrected by subtracting the respective MFI values from non-EV controls that were treated exactly like the

EV samples. The values of the corresponding isotype controls were also subtracted.

EV labeling and accumulation in tumor cells

EV have been labelled with PKH67 (PKH67GL-1KT Sigma-Aldrich) endowed with excitation at 490 nm and emission at 504 nm.

The labeling was carried out using the PKH67 Green Fluorescent Cell Linker Mini Kit for General Cell Membrane Labeling (Sigma-Aldrich) according to the manufacturer’s instructions. Samples were added with diluent C and PKH67 and subsequently 10% BSA/0.971 M sucrose. EV were then ultracentrifuged (100000xg) 1 h at 4 °C and resuspended in saline containing 1% DMSO.

The accumulation capability of PKH67GL-1KT-labeled EV in the mesothelioma cell line MSTO-211 H cells (ATCC, LGC standard, Milan, Italy) was evaluated by flow cytometric analysis. Cells were seeded in 12-well plates (12500 cells/cm²) and 48 h later they were exposed to two different concentrations of EV (7,2 × 10⁷ and 5,4 × 10⁶). Four or 24 h after treatment cells were harvested by trypsin-EDTA and resuspended in medium, i.e., RPMI-1640 (Sigma, St. Louis, Missouri, United States) containing 10% FBS (Euroclone, Milan, Italy). The cells were then washed with PBS and resuspended in 500 µL of PBS for flow cytometric analysis. Untreated cells were used as a control sample. Samples were acquired using the BD Accury flow cytometer (BD Accuri, Becton Dickinson, Milan, Italy). Ten thousand events were acquired for each sample. Data analysis was carried out using the Kaluza Analysis 2.1 software (Beckman Coulter Brea, California, United States). Fluorescence was expressed as MFI.

Paclitaxel dosage

The quantification of PTX was carried out as previously described [24]. The analysis was performed with an LC/MS 6546 platform that includes an Agilent 1290 II liquid chromatography system (Agilent Technologies, Palo Alto, CA, United States) coupled to a quadrupole-time-of flight (q-TOF) mass spectrometer (Agilent Technologies, Palo Alto, CA, United States). Chromatographic separation was performed with hydrophilic interaction liquid chromatography (HILIC) using an Acquity amide column, 100 × 2.1 mm, 1.7 µm (Waters, Milford, MA, USA), and the chromatographic eluents were as follows: A, 100% water, and B, 100% methanol, both containing 0.1% formic acid. The gradient applied was as follows: 0 min 80% of B, 3 min 2% of B, 3.1 min 20% of B, 4 min 80% of B, 6 min 80% of B. The flow rate was 0.25 mL/min, the column temperature was set at 45 °C and the injection volume was 15 µL. The samples were analyzed in ESI positive ionization mode, and the mass spectrometer was

operated at a resolving power of 40,000 over a full scan range of m/z 100–1200 at a scan rate of 2 spectra/s with the following settings: gas flow 10 l/min; gas temperature 180 °C; nebulized 50psi; sheath gas temperature 350 °C; sheath gas flow 11 l/min; capillary voltage 3500 V; nozzle voltage 1000 V; fragmentator 250 V. The quantification of PTX was assessed both in the isolated EV-PTX and in the EV-depleted supernatants, in both cases the detection and quantification of PTX was performed using the Na^+ adduct ion.

Isolated EV-PTX samples were processed as follows: 3 mL of cold methanol was added to 1 mL of EV samples. Then, samples were centrifuged at 15,000 \times g for 3 min at 4 °C, supernatants were dried and finally reconstituted with 80 μL methanol. Calibration curve was used for quantification spiking PTX to EV sample from 1 ng/mL to 100 ng/mL.

EV-depleted supernatants were processed as follows: 1 mL of cold methanol was added to 1 mL of medium sample. Then, samples were centrifuged at 15000 \times g for 3 min at 4 °C, supernatants were dried and finally reconstituted with 80 μL methanol. Calibration curve was used for quantification spiking PTX to medium sample from 1 ng/mL to 100 ng/mL. Some medium samples containing PTX were further diluted to fit the linear range 1ng/mL to 100 ng/mL.

Antiproliferative activity of EV-PTX (Potency)

The potency test evaluates the antiproliferative activity of EV-delivered PTX.

The effect of EV-PTX was evaluated in the pleural mesothelioma cell line NCI H2052 as a reference. NCI-H2052 cells were seeded in a 96-well culture plate (1000 cells/well in 100 μl). The cells were placed in an incubator at 37 °C and 5% CO_2 for 18–24 h to promote adhesion.

After 18–24 h, a curve with serial dilutions of PTX, in quadruplicate (25–0.4 ng/mL) was set up in complete MSC medium as diluent; EV/EV-PTX were added at 100 μL /well in triplicate (TEST); 100 μL /well of MSC (negative control, absence of PTX) and MSC-PTX (positive control, presence of PTX in free form and conjugated to EVs) supernatants were added in triplicate; 0 ng/mL PTX reference, consisting of complete MSC growth medium, was added, 100 μL /well, to fill the plate.

The plate was incubated for 7 days at 37 °C and 5% CO_2 . After 7 days of culture, the intensity of proliferation was evaluated by incubation of the plate with MTS at 37 °C for 2.5 ± 0.5 h; the absorbance was measured at 492 nm on a plate reader (Victor NIVO, Perkin Elmer).

The data were managed via GraftPad Prism software, version 10.2.3. A four-parameter logistic regression (4PL) function was applied for the analysis; the effect induced by EV/EV-PTX was quantified by comparison with the standard curve of pure PTX, plotted with respect to the

percentage of surviving cells (% viability), and expressed as Paclitaxel Equivalent Concentration of PTX (PEC, ng/mL).

Stability assessment

The stability of the fresh EV and EV-PTX was assessed ($n=3$ samples) in terms of EV number and size and EV surface markers under the following conditions: a) immediately at the end of ultracentrifugation ($t=0$), with samples maintained at RT; $t=0$, with samples maintained at 4 °C; 2.5 h after the end of ultracentrifugation ($t=2.5$), with samples maintained at RT; $t=2.5$, with samples maintained at 4 °C; and 12 h after the end of ultracentrifugation ($t=12$), with samples maintained at 4 °C.

The stability of the cryopreserved EV and EV-PTX was assessed ($n=6$ samples) in terms of EV number and size, total protein content and EV surface markers, and the product was thawed within 30 days of cryoconservation and at 6 and 12 months after freezing.

Impact of preprocessing storage of EV-containing supernatant

The impact of storing EV-containing supernatants on EV isolation/characterization was investigated. Specifically, three EV samples isolated immediately after supernatant collection were compared with those obtained after the storage of supernatants supplemented with or without 1% DMSO at -80 °C for 1 month.

Statistical analysis

Statistical analyses were performed via GraphPad Prism software, version 10.2.3. The quantitative data collected from independent experiments are expressed as the mean \pm standard deviations (SDs). Differences between two datasets were determined by Student's t test; two-way ANOVA was used for multiple comparisons. Statistical significance was accepted for p values < 0.05 (*), < 0.01 (**), or < 0.001 (***)

Results

MSC isolation and characterization

MSCs were isolated from a mean of 40 mL (range: 25–60 mL) of AT lipoaspirate collected from 13 healthy donors.

We were able to isolate MSCs from 13/13 processed lipoaspirate samples. MSCs sprouted from the lipoaspirates after a median time of 3.88 days (range: 3–5 days) and underwent the first detachment (P1) after a median time of 11.44 days (range: 7–14 days). The cells were expanded in flasks until a maximum P4 was reached.

MSC displayed the typical spindle-shaped morphology, as shown in Fig. 1A; PDT was 19.96 ± 4.62 h at P2, 21.18 ± 2.89 h at P3. Results are expressed as mean \pm SD of 13 cultures.

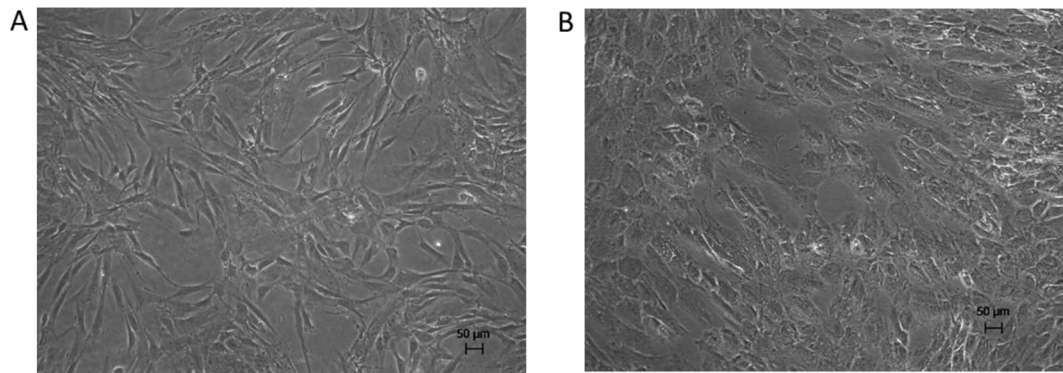


Fig. 1 MSCs morphology. (A) Spindle-shaped morphology of MSCs at P3; (B) MSCs morphology after loading with PTX. Magnification 10X

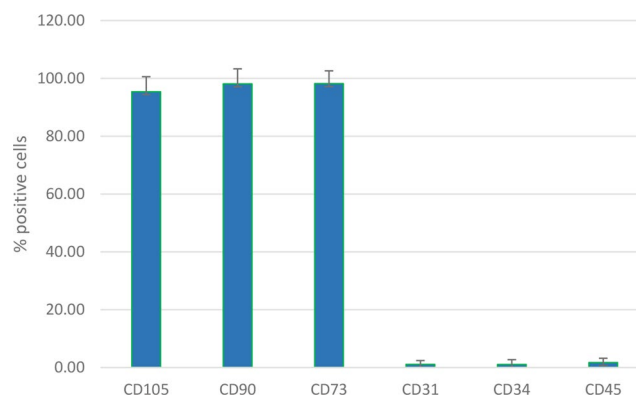


Fig. 2 Flow cytometry analysis of MSCs. Cells displayed high percentages of the typical MSCs-positive markers and are negative for hematopoietic and endothelial markers

During the culture period, the cells maintained a high percentage of viability, as evaluated with trypan blue staining at every passage (mean value $96.5 \pm 3.41\%$).

After a first expansion in flasks, MSCs displayed high percentages of the markers typically expressed by AT-derived MSCs (CD90 = $98.09 \pm 5.22\%$, CD105 = $95.36 \pm 5.21\%$ and CD73 = $98.18 \pm 4.43\%$) and were negative for hematopoietic markers (CD31 = $1.09 \pm 1.32\%$, CD34 = $1.03 \pm 1.7\%$ and CD45 = $1.7 \pm 1.5\%$, mean \pm SD, Fig. 2 and Supplementary Table S1).

After the PTX loading and starvation phases, the cells maintained plastic adhesion with a variation in morphology that ranged from spindle shaped to rounded (Fig. 1B). At the end of the culture period, the MSCs and MSC-PTX were harvested to evaluate the cell number and viability. Cell number was $7.60 \pm 2.85 \times 10^6$ MSCs and $6.78 \pm 4.29 \times 10^6$ MSCs-PTX, whereas viability was $96.18 \pm 2.67\%$ (MSCs) and $96.75 \pm 2.48\%$ (MSCs-PTX, mean \pm SD of 13 cultures, Supplementary Table S2).

Assessment of EV and EV-PTX identity

Number, size, protein content and morphology

Starting from $7.60 \pm 2.85 \times 10^6$ MSCs (mean \pm SD of 13 samples) at 50–60% confluence in 80 mL supernatants,

we were able to obtain $7.03 \pm 6.55 \times 10^9$ total EV particles (mean \pm SD). All EV samples analyzed with a NanoSight NS300 system presented a single peak and a very homogeneous population, with sizes ranging from 186 to 263 nm (Fig. 3A and Supplementary Table S3). The EV protein content was $40.19 \pm 13.30 \mu\text{g/mL}$ (mean \pm SD of $n = 13$ samples). Finally, as recommended by the MISEV guidelines, a selected number of EV samples were evaluated using high-resolution imaging technique (TEM). The morphology of the EVs exhibited the characteristic lipid bilayer and confirmed their round-shaped structure. (Fig. 4A).

The number of EV-PTX was not significantly different from that of EVs. Starting from $6.78 \pm 4.29 \times 10^6$ MSCs-PTX (mean \pm SD of 13 samples) at 50–60% confluence in 80 mL supernatants, we were able to obtain $5.92 \pm 2.92 \times 10^9$ total particles (mean \pm SD). All EV-PTX analysis showed a single peak and a very homogeneous population, with sizes ranging from 189 to 248 nm (mean 213 nm), very similar to those of EVs. (Fig. 3B and Supplementary Table S3). The protein content of EV-PTX was $44.90 \pm 15.73 \mu\text{g/mL}$. The integrity, morphology and size of EV-PTX were confirmed via TEM (Fig. 4B).

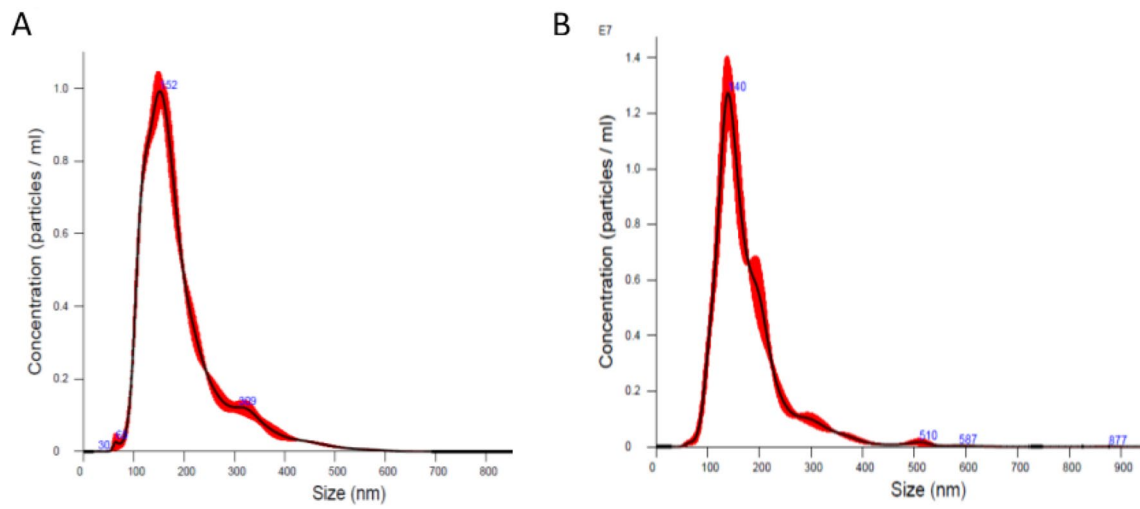


Fig. 3 EV characterization by NTA. Analysis of a representative sample of EV (A) and the corresponding EV-PTX (B). Both EV and EV-PTX showed a single peak and a very homogeneous population

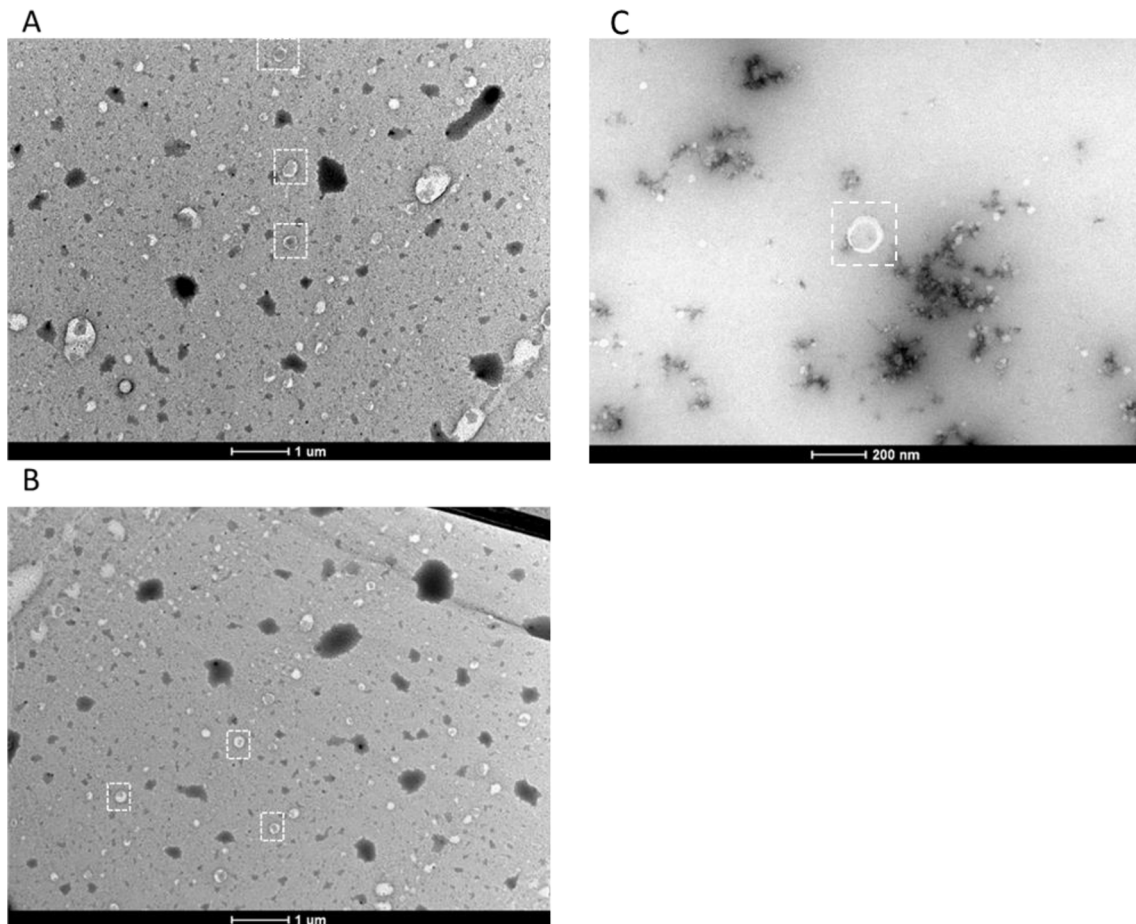


Fig. 4 EV characterization by TEM. EV (A) and EV-PTX (B) morphology by TEM analysis. White dotted squares highlight three representative examples of EV and EV-PTX among many others. Panel C show a high magnification (200 nm) image of an EV, underlining the lipid bilayer structure

Flow cytometry analysis of exosome surface markers

Flow cytometry analysis confirmed the expression of the tetraspanins CD9, CD63 and CD81 in both the EV and EV-PTX samples. The typical AT-derived MSC surface markers CD105, CD49e, CD146, CD44, and CD29 were also highly expressed in both the EV and EV-PTX samples. Specific leucocyte markers (CD1c, CD2, CD3, CD4, CD8, CD14, CD19, CD20, and CD56) and platelet markers (CD41b, CD42a, and CD62p), as well as the endothelial marker CD31, were present only at very low levels on the EV and EV-PTX surfaces. (Fig. 5A). The Figure shows slightly greater expression of the typical MSC-positive markers CD105, CD49e, CD44 and CD29 in EV-PTX samples than in EV samples, although the differences

were not significant. Figure 5B show the comparison of the proportion of EV positive for MSC markers with those positive for platelet markers in terms of normalized CD9/CD63/CD81 median signal intensity (%).

Cytofluorimetric analysis of EV accumulation

PHK67-stained EVs were used to evaluate EV accumulation in MSTO-211 H cells. The cells were exposed to 2 different concentrations of EV and analyzed after 4–24 h, as shown in Fig. 6. Under these conditions, we observed increased fluorescence compared with the autofluorescence of untreated control cells, already at 4 h (Panel A), with a higher concentration of EVs (7.2×10^7 EV) corresponding to a ratio of approximately 5900 EV/cell,

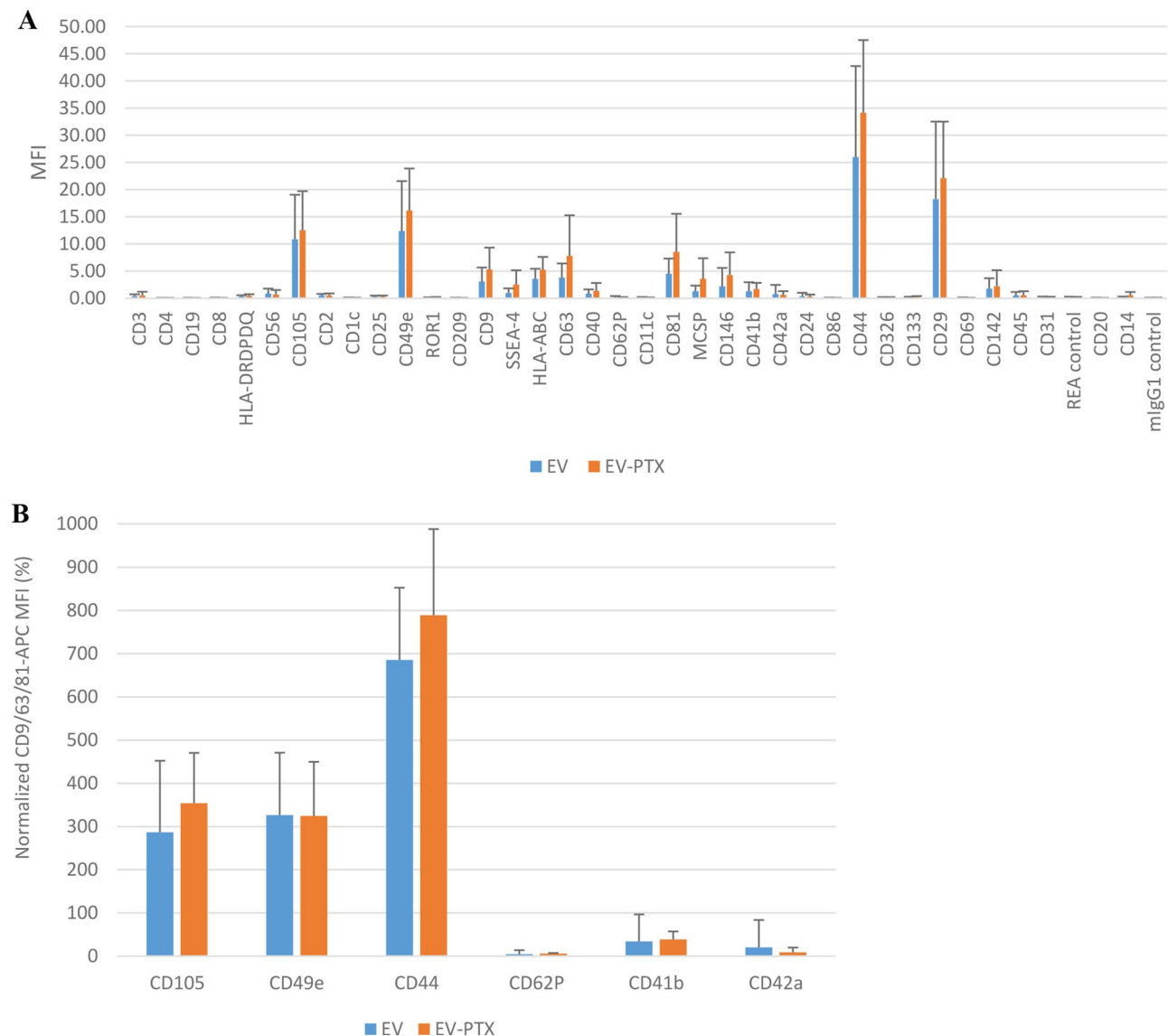


Fig. 5 EV characterization by flow cytometry analysis. (A) Both EV and EV-PTX show high expression of the tetraspanins CD9, CD63 and CD81 as well as of the typical MSC markers CD105, CD49e, CD146, CD44, and CD29; (B) comparison of the proportion of EV positive for MSC markers with those positive for platelet markers in terms of normalized CD9/CD63/CD81 median fluorescence intensity (%). MFI, Median Fluorescence Intensity

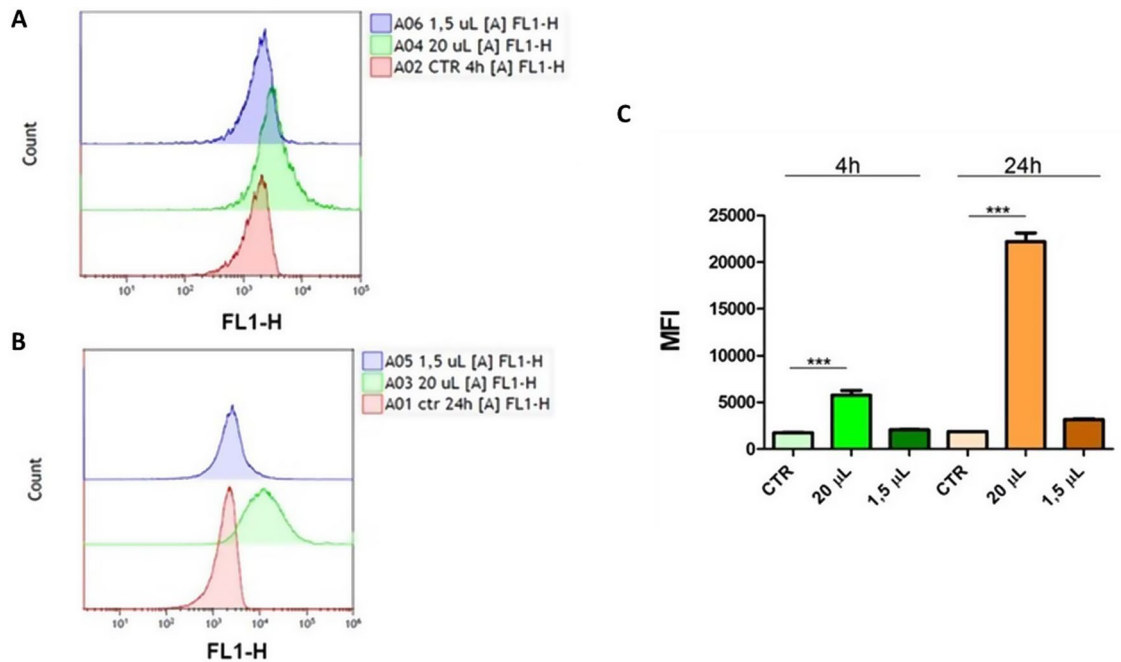


Fig. 6 Quantitative analysis of accumulation of EVs in MSTO-211 H cells. Cells were seeded and treated 48 h later with EVs at the concentration of 7.2×10^7 (20 μ L) or 5.4×10^6 (1.5 μ L) for 4–24 h (Panel A and B, respectively). EV accumulation was evaluated by flow cytometry measuring and quantifying the MFI in panel C. Statistical analysis was performed using ANOVA followed by Bonferroni’s test. $P < 0.001$ ***

whereas with a lower concentration of EVs, the increase in fluorescence was negligible. A more marked accumulation of EVs was observed after 24 h of incubation (Panel B). MFI quantification and statistical analysis are reported in Figure ($P < 0.001$ OneWay ANOVA followed by Bonferroni’s test).

Paclitaxel dosage

To determine the quantity of PTX released by the MSC inside the EV or in a “free-form”, the quantification of PTX was assessed both in the EV-PTX and in the EV-PTX-depleted supernatants.

PTX content was $8.11 \pm 0.1 \times 10^{-5}$ ng/ 10^6 EV.

(mean \pm SD). The concentration of PTX in the EV-PTX-depleted supernatants was 36.18 ± 13.82 ng/mL. As expected, we detected no evidence of PTX in the unloaded EVs or in the EV-depleted supernatants, which were used as controls.

Antiproliferative activity of EV-PTX (Potency)

To evaluate the amount of pharmacologically active PTX incorporated by EV-PTX, isolated EV-PTX, whole EV-PTX-containing supernatants (SUP#1) and EV-PTX-depleted supernatants (SUP #2) were tested for their ability to inhibit the proliferation of the pleural mesothelioma cell line NCI H2052; the PTX content was indirectly quantified by its cytostatic effect. EV-PTX and supernatants were compared to the unloaded EV/supernatant (as background), which was produced following

Table 2 Antiproliferative activity of EV-PTX and supernatants

	NO PTX (background)		PTX	
	PEC ng/mL	% Viability	PEC ng/mL I	% Viability
EV	3.234 \pm 0.092	86.8 \pm 0.8	4.616 \pm 0.336	76.0 \pm 2.9
SUP #1	3.795 \pm 1.146	88.2 \pm 13.1	12.227 \pm 2.471	26.8 \pm 7.2
SUP #2	4.248 \pm 0.687	78.2 \pm 6.4	11.236 \pm 3.239	32.4 \pm 17.7

Antiproliferative activity of EV-PTX and supernatants compared with that of unloaded EVs/supernatants. EV-PTX had a significantly greater effect when compared to PTX-unloaded EV ($p = 0.02110$ PEC, $p = 0.02636\%$ survival). EV-PTX showed a significantly lower cytostatic effect when compared to both SUP#1 and SUP#2 (vs. SUP#1 $p = 0.00358$ PEC, $p = 0.00012\%$ survival; vs. SUP#2 $p = 0.01850$ PEC, $p = 0.00927\%$ survival). No statistically significant differences are detected between SUP#1 and SUP#2. PTX, Paclitaxel; SUP, Supernatant; EV, Extracellular Vesicles; PEC, Paclitaxel Equivalent Concentration

the same manufacturing process. As shown in Table 2, EV-PTX had a significantly greater effect when compared to PTX-unloaded EV ($p = 0.02110$ PEC, $p = 0.02636\%$ survival), thus demonstrating that the PTX incorporated into EVs is pharmacologically effective.

However, the isolated EV-PTX showed a significantly lower cytostatic effect when compared to both SUP#1 and also SUP#2 (vs. SUP#1 $p = 0.00358$ PEC, $p = 0.00012\%$ survival; vs. SUP#2 $p = 0.01850$ PEC, $p = 0.00927\%$ survival). No statistically significant differences were detected between SUP#1 and SUP#2.

The majority of the biological effects appear to be concentrated in the supernatants, even in the EV-PTX-depleted portion (SUP#2), thus suggesting that most of the PTX is released from MSCs in free form.

Stability assessment

The stability of the fresh EV/EV-PTX was evaluated in terms of particle number and size, and the results are presented in Table 3.

No significant differences were observed when the samples were maintained at either RT or 4 °C for up to 2.5 h after EV isolation. Moreover, the tested parameters remained stable for up to 12 h when the EVs were stored at 4 °C. Similar findings were obtained from the EV-PTX analysis.

Flow cytometry analysis revealed that EV and EV-PTX samples maintained similar expression of the typical MSC surface markers CD105, CD49e, CD44, and CD29

for up to 2.5 h after isolation, either at RT or at 4 °C; a decrease in the expression of the typical MSC markers was observed after 12 h keeping EV at 4 °C, although the differences were not significant. (Fig. 7A-D)

The same stability study was performed on EV and EV-PTX samples stored at -80 °C for 1, 6 and 12 months. All the evaluated parameters remained unchanged for up to 12 months of cryoconservation, as reported in Table 4 for particle number and size and in Fig. 8A-B for the typical MSC surface markers.

Impact of the EV-containing supernatant storage conditions

To evaluate whether the storage conditions of EV-containing supernatants affect EV isolation and characterization, three EV samples isolated immediately after supernatant collection (fresh SUP) were compared with those obtained after the storage of the supernatant, supplemented or not supplemented with 1% DMSO (SUP-Cryo-DMSO versus SUP-Cryo), at -80 °C for 1 month.

Processing a volume of 43 mL of supernatants, we were able to obtain $9.79 \pm 4.01 \times 10^9$ EVs from fresh SUP, $4.50 \pm 3.38 \times 10^9$ EVs from SUP-Cryo-DMSO and $4.90 \pm 4.6 \times 10^9$ EVs from SUP-Cryo. The EV sizes obtained under the three conditions were similar: 213.1 ± 8.6 nm in fresh SUP, 203.3 ± 8.3 nm in SUP-Cryo-DMSO, and 188 ± 9.1 nm in SUP-Cryo (mean \pm SD of 3 runs, Supplementary Table S4). These differences were not statistically significant. NTA graphs of a representative EV sample treated under the three conditions are shown in Fig. 9 (A-C).

Flow cytometry analysis (Fig. 10) revealed greater expression of typical MSC surface markers in EVs obtained from fresh SUP than in those derived from cryopreserved SUP-Cryo. A significant reduction in the expression of the markers CD44 ($p < 0.01$) and CD29 ($p < 0.05$) was observed.

In contrast, no statistically significant differences were found between fresh SUP and SUP-Cryo-DMSO, although slightly lower expression of the MSC-positive markers CD105, CD49e, CD44 and CD29 was noted in SUP-Cryo-DMSO.

Characterization of EVs from platelet lysates

To better characterize our final product, i.e. EVs and EV-PTX obtained from MSCs and to exclude the presence of EVs of plasma origin, we analyzed EVs obtained from fresh complete medium containing platelet lysate at the same concentration used for MSC culture, following the same EVs isolation protocol as that used for MSC-derived EVs.

Platelet lysate-derived EVs were characterized in terms of particle number, size and surface marker expression. Starting from 30 mL of complete medium

Table 3 Stability of the fresh product

EV	Number-RT (particle/mL)	Number- T=4 °C (particle/mL)	Size-RT (nm, mean \pm SD)	Size-4 °C (nm, mean \pm SD)
HD 1 t=0	3.30×10^9	3.80×10^9	205.4 ± 108.6	184.1 ± 88.7
HD 1 t=2,5 h	2.50×10^9	3.30×10^9	210.3 ± 97.9	200.5 ± 105.3
HD 1 t=12 h	/	3.62×10^9	/	177.2 ± 89.3
HD 2 t=0	7.52×10^9	9.08×10^9	188.4 ± 85.4	181.6 ± 86.1
HD 2 t=2,5 h	9.81×10^9	1.18×10^{10}	178.4 ± 76.3	181.2 ± 82.2
HD 2 t=12 h	/	7.95×10^9	/	192.8 ± 88.4
HD 3 t=0	8.58×10^9	7.54×10^9	189.9 ± 95.7	189.2 ± 95.8
HD 3 t=2,5 h	7.29×10^9	6.76×10^9	191 ± 91.1	192.4 ± 93.9
HD 3 t=12 h	/	6.97×10^9	/	194.3 ± 91
EV-PTX				
HD 1 t=0	2.30×10^9	2.80×10^9	187 ± 90.4	182.3 ± 84.7
HD 1 t=2,5 h	2.10×10^9	2.70×10^9	207.4 ± 107	192.2 ± 91.8
HD 1 t=12 h	/	2.65×10^9	/	192.8 ± 91.1
HD 2 t=0	5.00×10^9	4.70×10^9	197.1 ± 100.5	207 ± 97.2
HD 2 t=2,5 h	3.66×10^9	4.32×10^9	195.5 ± 96.3	195.7 ± 97.1
HD 2 t=12 h	/	4.11×10^9	/	194.6 ± 98.3
HD 3 t=0	4.86×10^9	6.44×10^9	222.8 ± 110.9	206.7 ± 105.9
HD 3 t=2,5 h	5.30×10^9	5.53×10^9	211.2 ± 109	217.4 ± 101.9
HD 3 t=12 h	/	5.13×10^9	/	234.5 ± 102.5

Stability assessment of the fresh product in terms of number and size. HD, Healthy Donor; T, Temperature; RT, Room Temperature; EV, Extracellular Vesicles; PTX, Paclitaxel; SD, Standard Deviation; nm, nanometer

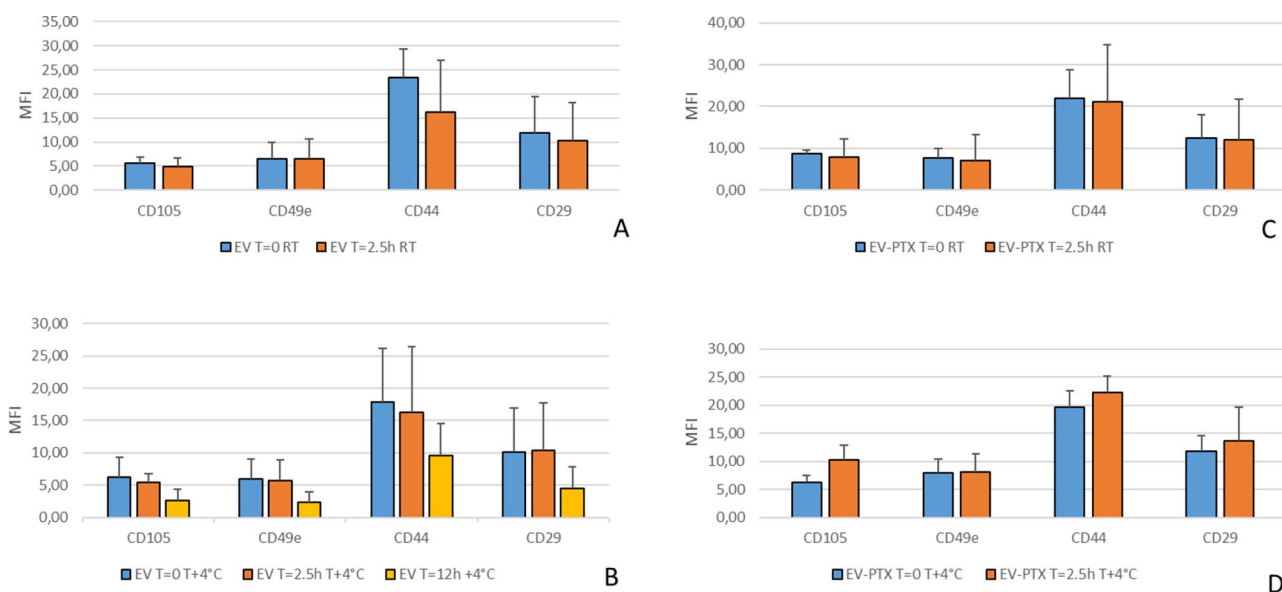


Fig. 7 Stability assessment of the fresh product by flow cytometry analysis. EV samples maintain a similar expression of the typical MSCs surface markers CD105, CD49e, CD44, and CD29 up to 2,5 h after isolation, preserving EV both at room temperature (A) and at +4 °C (B); a decrease in the expression of the typical MSCs markers was observed 12 h after EV isolation keeping EV at +4 °C (B), although the differences were not significant. Similar results were obtained analyzing EV-PTX at room temperature (C) and at +4 °C (D). MFI, Median Fluorescence Intensity

Table 4 Stability of the cryopreserved product

	< 1 month	6 months	12 months
EV Number (particle/mL)	5.89 ± 1.77 × 10 ⁹	3.44E ± 1.7 × 10 ⁹	6.11 ± 2.92 × 10 ⁹
EV Size (nm)	213.34 ± 12.95	216.38 ± 28.92	187.94 ± 8.81
EV-PTX Number (particle/mL)	8.59 ± 3.34 × 10 ⁹	6.71 ± 4.23 × 10 ⁹	8.14 ± 4.08 × 10 ⁹
EV-PTX Size (nm)	218.84 ± 19.97	209.24 ± 7.71	202.45 ± 11.68

Stability assessment, in terms of number and size, of the products cryopreserved for < 1 month, 6 months and 12 months. EV, Extracellular Vesicles; nm, nanometer

containing 1.5 mL of platelet lysate, we were able to obtain $2.05 \times 10^{10} \pm 4.95 \times 10^9$ total EV particles (mean ± SD of 6 runs, Supplementary Table S5). All EV analyses revealed a single peak and a very homogeneous population, with a size of 144.62 ± 9.19 nm (mean ± SD, Supplementary Table S5). Figure 11 displays the analysis of a representative sample.

Flow cytometry analysis of platelet-derived EVs confirmed high expression of the typical platelet markers HLA-ABC, CD62P, CD41b, CD42a, and CD29, whereas the typical MSC surface markers CD105, CD44, and CD49e were present at very low levels (Fig. 12A-B, respectively).

Discussion and conclusions

There is currently no consensus on best practices for any of the critical stages in obtaining MSC-derived EVs. An opinion paper by members of several scientific societies

focused on EVs reported that many factors can affect EVs quantitatively and qualitatively [25]. Differences in sample collection, MSC sources, culture conditions and media used, as well as in EV isolation and collection and storage strategies, may lead to the generation of products with different features and functional activity [19, 26, 27].

In the present study, we aimed to explore the possibility of setting up a GMP-compliant protocol for the preparation of MSC-EVs, starting from AT lipoaspirates from healthy donors, and to investigate the feasibility of preparing EVs loaded with PTX for potential clinical application as drug products.

Different groups believe that a critical issue to obtain MSC-EV compliant, in terms of quantity and quality, is the compliance of the MSC [25, 28, 29]. We previously demonstrated the possibility of generating highly standardized, large-scale, GMP-compliant MSCs, also loaded with the chemotherapeutic drug PTX and that our approach was efficient in terms of quantity and quality of the obtained medicinal product [22]. Regulatory agencies approved the Investigational Medicinal Product Dossier and in the year 2022 authorized the Facility of the IRCCS Neurological Institute C. Besta Foundation for the MSC production process and quality controls. The protocol of the clinical trial (PacliMES, Eudract number 2020-005928-11), aimed to treat patients with pleuric malignant mesothelioma was also approved [20]. In this protocol the drug is administrated locally. The clinical efficacy of a drug is highly dependent on the administration route. Historically, systemic delivery has been the most widely used method in cancer patients, but the

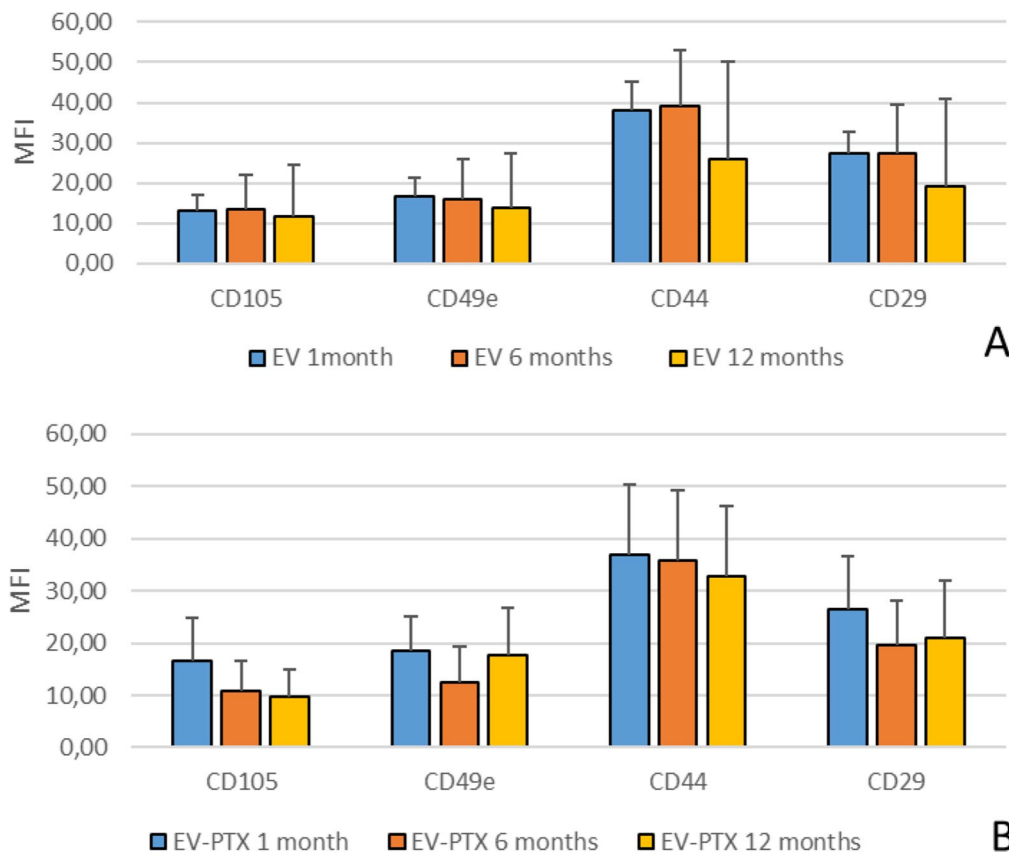


Fig. 8 Stability assessment of the cryopreserved product by flow cytometry analysis. **(A)** Analysis of EV samples at time points $t \leq 1$, $t = 6$, $t = 12$ months after cryoconservation; **(B)** Analysis of EV-PTX at time points $t \leq 1$, $t = 6$, $t = 12$ months after cryoconservation. No significant differences were found at different time points both in EV and EV-PTX. MFI, Median Fluorescence Intensity

results have often been disappointing. After intravenous injection, the amount of drug that reach the tumor site is low and consequently the therapeutic effect is reduced. Moreover, increasing the dose to achieve better efficacy is often not possible due to the risk of systemic toxicity. To overcome this hurdle and to localize the drug’s effect at the tumor site, while sparing normal tissue and minimizing collateral toxicity, local delivery should be the preferred route of administration although it is rarely feasible. Peculiar characteristics of the MSC, as well as of the MSC-derived EV, include their tumor-specific homing capability and their ability to release anti-inflammatory molecules. Therefore, EV-PTX delivery can be envisioned both locally, for intraperitoneal or intrapleural tumors, and systemically [20].

This highly standardized MSC production process represented the background from which we started the present study. The results of the characterization of MSCs obtained from the 13 healthy volunteers confirmed those previously reported. Another critical issue in the MSC-derived EV preparation process is the use of platelet lysate as supplement of the MSC culture medium; this is an almost imperative choice to avoid the use of

serum, especially of animal origin, during MSC culture, as requested from the regulation for drug product manufacturing. However, as described by different groups, platelet lysate contains EVs of plasma origin, therefore the final product obtained at the end of the MSC-derived EV preparation process also contains EVs of plasma origin [25, 30–32]. We introduced, in our protocol, 24 h of MSC culture (not exceeding 50–60% confluence) without platelet lysate before supernatant collection to deprive supernatants from EVs of plasma origin and to stimulate the maximum EV release from MSCs, as suggested by different studies [25, 32, 33]. To demonstrate that the EVs isolated with our protocol were derived from MSCs and not from plasma and to better characterize our product, we analyzed EVs obtained from complete medium alone, following the same isolation protocol as that used for MSC-derived EVs. The results revealed that platelet lysate-derived EVs are slightly smaller than MSC-derived EVs and, most importantly, highly express the typical platelet markers HLA-ABC, CD62P, CD41b, and CD42a and low levels of the typical MSC markers CD105, CD44 and CD49e. Conversely, EV-derived MSCs displayed very low levels of platelet markers and high levels of MSC

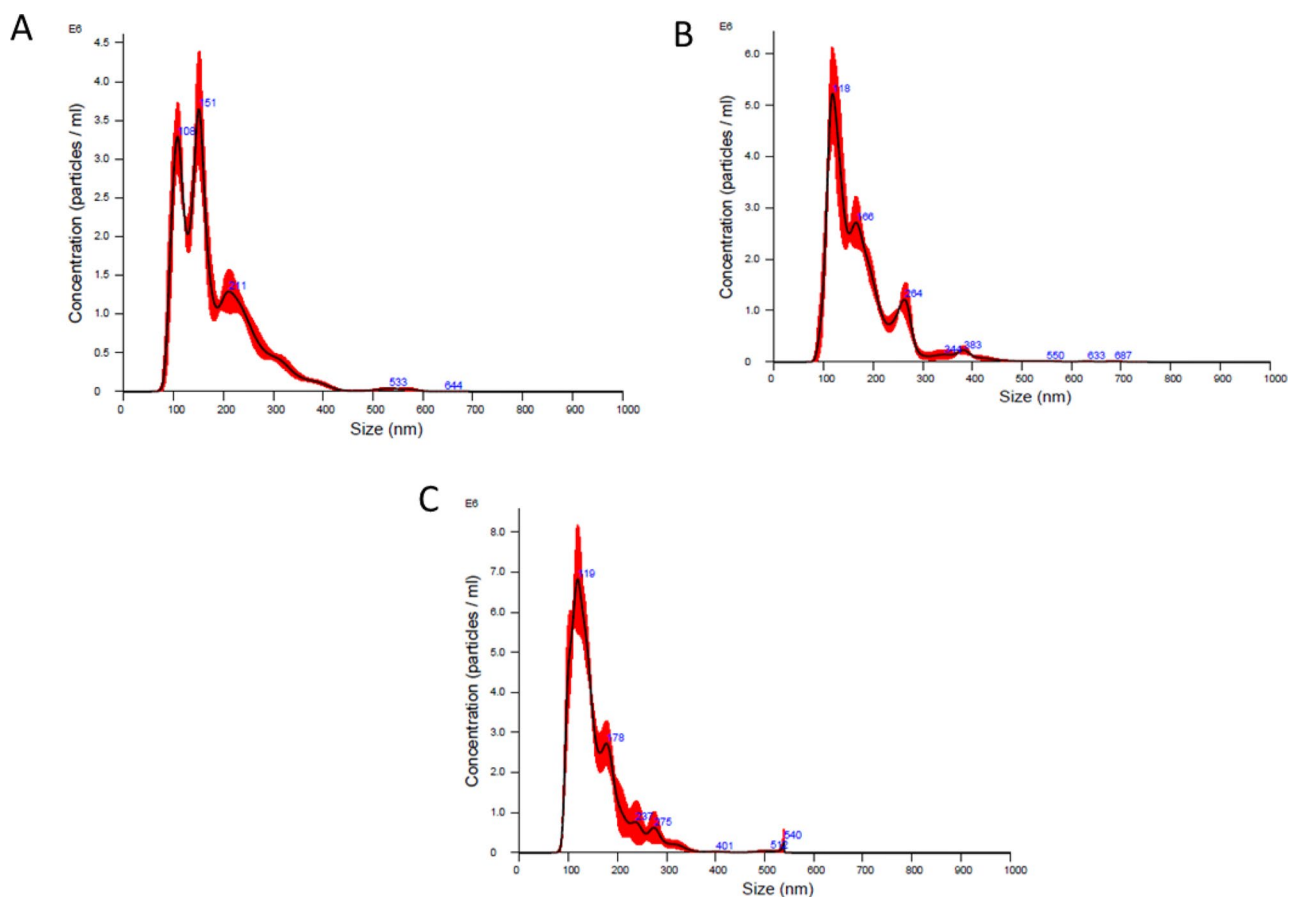


Fig. 9 Impact of pre-processing storage of EV-containing supernatant-NTA analysis. Analysis of a representative EV sample isolated immediately after supernatants collection (fresh SUP, **A**) compared with those obtained after the storage of supernatant, supplemented with 1% DMSO (SUP-Cryo-DMSO, **B**) or alone (SUP-Cryo, **C**)

markers. This finding allows us to exclude the presence of platelet lysate-derived EVs in the final product.

EV and EV loaded with PTX were similar in terms of morphology, number, size and distribution, as evaluated by TEM and NTA. Moreover, the EV/EV-PTX population is very homogeneous. Flow cytometry analysis confirmed the expression of tetraspanins and typical AT-derived MSC surface markers in both the EV and EV-PTX samples, with slightly but not significantly greater expression of all positive markers in the EV-PTX samples than in the EV samples. Taken together, these results confirmed the identity of our EV products.

The results of the stability assessment in terms of identity, number and size of the fresh EV/EV-PTX demonstrated that EV (both PTX loaded and unloaded) maintained their concentration/integrity and cytofluorimetric profile up to 2.5 h from the isolation, when preserved at a temperature of 4 °C and at room temperature. When maintained at a temperature of 4 °C, EVs are stable for up to 12 h, although a moderate, not significant decrease in the expression of typical MSC markers was observed. In terms of long-term stability, EV/EV-PTX cryopreserved

at -80 °C maintained their identity, concentration and integrity for up to 12 months.

Considering that the management of the manufacturing processes within the Facilities can be difficult, especially in the case of small multiproduct Facilities with a limited number of Class B suites, as is the case of a public hospital Facility, the possibility of cryopreserving the EV-containing conditioned medium (at the end of the cell culture process and before the EV/EV-PTX isolation) was evaluated. There is no consensus on this issue, with some laboratories showing that preprocessing storage conditions are not critical for EV isolation [34–36] and others showing that freeze/thaw damage occurs, implying that cryopreservation and proper storage temperatures are important [37–40]. EV isolated immediately after supernatant collection (fresh SUP) were compared with those isolated from the supernatant cryopreserved in the presence or absence of 1% DMSO (SUP-Cryo-DMSO and SUP-Cryo) at -80 °C for one month. NTA revealed a decreased concentration of EVs obtained from cryopreserved supernatants compared with those isolated from fresh samples, which also revealed increased expression

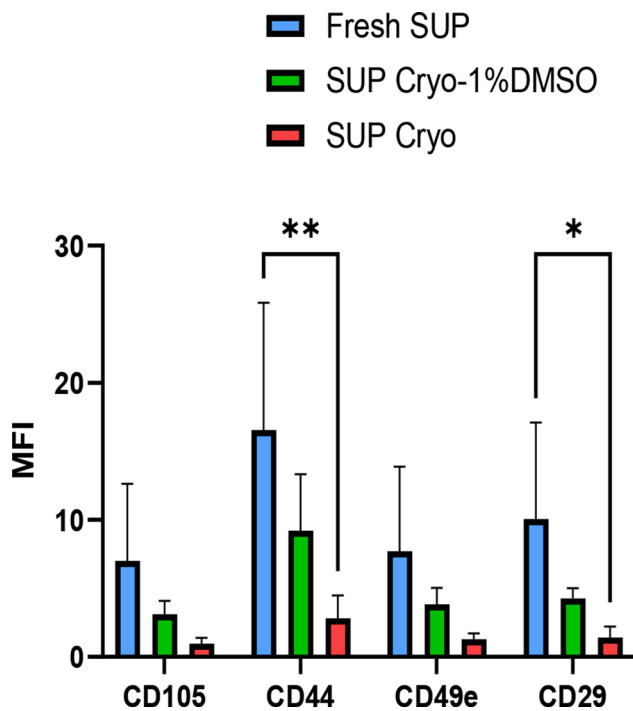


Fig. 10 Impact of pre-processing storage of EV-containing supernatant-Flow Cytometry Analysis. Supernatants processed immediately after collection (fresh SUP, blue) show higher expression of the typical MSCs surface markers than both supernatants cryopreserved supplemented of 1% DMSO (SUP Cryo-1% DMSO, green) and alone (SUP Cryo, red) at the temperature of -80 °C for 1 month. Samples cryopreserved alone displayed a significant reduction, in comparison with fresh SUP, in the expression, in terms of MFI, of the markers CD44 (** $p < 0,01$) and CD29 (* $p < 0,05$). Statistical analysis was performed using 2way ANOVA followed by Bonferoni's test. Greenhouse-Geisser method was used to apply corrections for multiple comparisons. MFI, Median Fluorescence Intensity

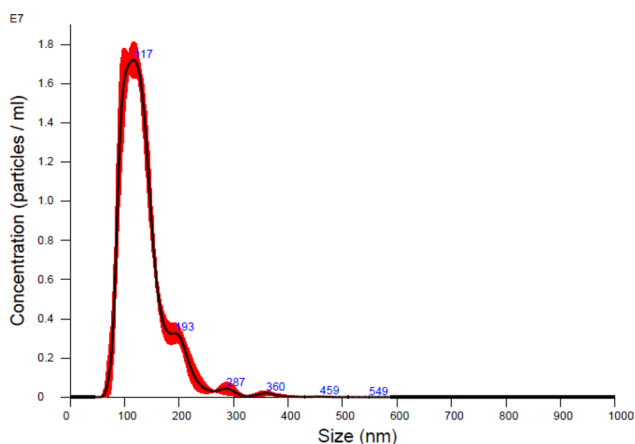


Fig. 11 Characterization of EV from platelet lysate-NTA analysis. The peak of a representative EV sample from platelet lysate show a very homogeneous population in terms of size

of typical MSC surface markers. Specifically, a significant reduction in the expression of the CD44 and CD29 markers was observed in the EVs isolated from supernatants cryopreserved in the absence of DMSO (SUP-Cryo).

These findings indicate that storing the EV-containing supernatant before EV isolation, especially in the absence of DMSO, is not recommended.

Concerning the feasibility of employing EVs as carriers for PTX delivery, our results demonstrate the ability of PKH67GL-1KT-labeled EVs to accumulate in the mesothelioma cell line MSTO-211 H; moreover, EVs loaded with PTX have the ability to incorporate the drug, as confirmed by PTX quantification, and release it. The released drug maintains its antiproliferative activity against the pleural mesothelioma cell line NCI H2052. As expected and also described by other groups [41]– [42], PTX is partially released encapsulated within EV and partially in a free form, as PTX was detected both in EV-PTX samples and in EV-PTX depleted supernatants.

EV-PTX demonstrated a significantly lower antiproliferative effect than that shown by the corresponding supernatants. However, it is important to highlight that EV-PTX effect is higher and statistically different from unloaded EV, demonstrating that PTX incorporated into EV is pharmacologically effective. The majority of pharmacological effect is concentrated in the supernatants, even in the EV-depleted portion, suggesting that most of the PTX is released from MSCs in free form.

Given these results, to obtain a biological effect from EV-PTX, comparable to that from whole EV-containing supernatant, it is necessary to use a number of vesicles that, from a productive point of view, could be difficult to obtain. The low efficiency in PTX loading may be associated with its high hydrophobicity and poor solubility in water. However, introducing some modifications in the manufacturing protocol could improve the efficiency of EV loading with PTX. A report from Kim and colleagues demonstrated that reducing the stiffness of exosome membranes by sonication promoted the incorporation of PTX into lipid bilayers, resulting in high loading capacity [43]. Moreover, post-isolation EV loading and sonication could increase cargo efficiency potentially allowing a lower number of EVs to achieve the desired biological activity. Alternative delivery strategies have recently been investigated such as nanocarriers for combination therapy in tumors, albumin bound PTX, or polymeric, lipid-based, and inorganic nanoparticles [44–48]. Nevertheless, the use of EVs as drug delivery tools for anti-cancer therapies, including conventional chemotherapy agents and novel RNA-based drugs, remains a promising hypothesis and a highly active area of research [49]– [50]. Certainly, increasing the cargo capacity of EVs thus reducing the required dose for infusion, is particularly important when EVs are produced by Academic Cell Factories. These facilities typically have a limited number of Class B clean rooms, a small workforce, and constrained budgets. Such Cell Factories are often engaged in multiple, relatively time-consuming production processes.

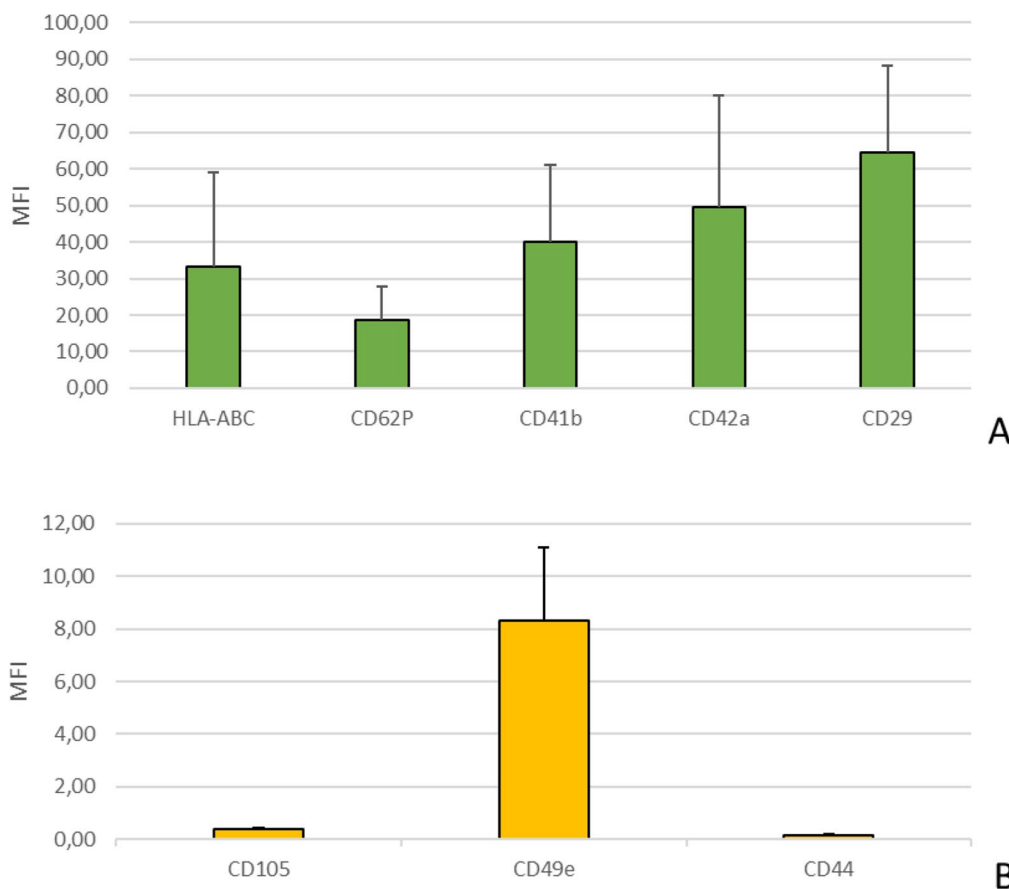


Fig. 12 Characterization of EV from platelet lysate-Flow cytometry analysis Samples show high expression of the typical platelet markers HLA-ABC, CD62P, CD41b, CD42a, CD29 (Panel **A**), and low expression of the typical MSC markers CD105, CD49e and CD44 (Panel **B**). MFI, Median Fluorescence Intensity

As a result, they face a choice: either concentrate their efforts on manufacturing a single product or invest in expanding both space and personnel. In addition to logistical challenges, another major limiting factor for these innovative therapies is the high production cost, which necessitates fundraising efforts. Overall, the results of this study indicate that, starting from AT lipoaspirate, our manufacturing protocol permits the use of GMP-compliant standardized MSC-EVs as carriers for PTX delivery. Further studies, mainly aimed to determine the optimal EV-PTX dosage, are mandatory to establish the use of the EV-PTX drug product in antitumor therapy.

Abbreviations

EV	Extracellular vesicles
MSC	Mesenchymal stromal cells
DDS	Drug delivery system
GMP	Good manufacturing practice
PTX	Paclitaxel
AT	Adipose tissue
DMEM	Dulbecco's modified medium
P	Passage
PDT	Population doubling time
CD	Clusters of differentiation
DMSO	Dimethyl sulfoxide

SUP	Culture supernatants
NTA	Nanoparticle tracking analysis
PBS	Phosphate buffer salt
TEM	Transmission electron microscopy
MFI	Median fluorescence intensity
BSA	Bovine serum albumin
EDTA	Ethylenediaminetetraacetic acid
PEC	Paclitaxel equivalent concentration

Supplementary Information

The online version contains supplementary material available at <https://doi.org/10.1186/s13287-025-04435-x>.

Supplementary Material 1

Acknowledgements

Not Applicable.

Author contributions

AM and ES: conceived and designed the study, performed cell cultures, collected and interpreted the data, wrote original draft; SN provided techniques and experimental validation, performed potency tests, analyzed and interpreted the data; GMS, AGC and CT: provided project management and resources, review and revised manuscript; PP, LM and GLB: performed the experiments of vesicles labelling and accumulation in tumor cells, analyzed and interpreted the data; SP, SF and PG: performed vesicles isolation and characterization tests; FM and FAC: performed the vesicles characterization

by TEM, analyzed and interpreted the data, provided funding; GM: provided starting material, reviewed and edited the manuscript; GP: performed vesicles characterization by HPLC, analyzed and interpreted the data, reviewed and edited the manuscript; DL: conceived and designed the study, collected and interpreted the data, provided funding and review and substantively revised manuscript. All authors have read and approved the manuscript. All authors agreed both to be personally accountable for the author's own contributions and to ensure that questions related to the accuracy or integrity of any part of the work, even ones in which the author was not personally involved, are appropriately investigated, resolved, and the resolution documented in the literature.

Funding

This research was supported by the Italian Ministry of Health and IRCCS Neurological Institute C. Besta Foundation (Ricerca Corrente to DL) and by Regione Lombardia POR FESR 2014–2020 “FORCE4CURE” Project-ID 2526393, as well as by the Italian Ministry of Health (grant number RRC) to FM.

Data availability

All data relevant to the study are included in the article or uploaded as Supplementary Tables.

Declarations

Ethics approval and consent to participate

Samples were collected after signed informed consent of no objection for the use for research of surgical tissues in accordance with the Declaration of Helsinki. The informed consents were obtained prior to tissue collection. The project was approved by ethical committee: *Title of the approved project*: “human Mesenchymal Stromal Cells (MSCs) loaded with drugs and derived Extracellular Vesicles: production process optimization and drug product characterization”. *Name of the institutional approval committee*: Institutional Review Board of the IRCCS Neurological Institute C. Besta Foundation. *Approval number*: 15. *Date of approval*: March 29, 2023. Human cell lines MSTO-211 H and NCI H2052 were purchased from a commercial vendor, ATCC. The company has confirmed that there was initial ethical approval for the collection of human materials and the derivation of cell lines and that the donors had signed informed consent. See for details: <https://www.atcc.org/products/crl-2081>; <https://www.atcc.org/products/crl-5915>.

Competing interests

The authors declare that they have no conflicts of interest. The funders had no role in the design of the study; in the collection, analyses, or interpretation of data; in the writing of the manuscript; or in the decision to publish the results. The authors declare that they have not use AI-generated work in this manuscript.

Received: 26 February 2025 / Accepted: 9 June 2025

Published online: 15 June 2025

References

1. Asadi K, Amini A, Gholami A. Mesenchymal stem cell-derived exosomes as a bioinspired nanoscale tool toward nextgeneration cell-free treatment. *J Drug Deliv Sci Technol.* 2022;77:103856.
2. Lyu C, Sun H, Sun Z, Liu Y, Wang Q. Roles of exosomes in immunotherapy for solid cancers. *Cell Death Dis.* 2024;15(2):106.
3. Soler-Botija C, Monguió-Tortajada M, Munizaga-Larroude M, Gálvez-Montón C, Bayes-Genis A, Roura S. Mechanisms governing the therapeutic effect of mesenchymal stromal cell-derived extracellular vesicles: A scoping review of preclinical evidence. *Biomed Pharmacother.* 2022;147:112683.
4. Lai RC, Yeo RW, Tan KH, Lim SK. Exosomes for drug delivery - a novel application for the mesenchymal stem cell. *Biotechnol Adv.* 2013;31(5):543–51.
5. Zhao W, Li K, Li L, Wang R, Lei Y, Yang H, et al. Mesenchymal stem Cell-Derived exosomes as drug delivery vehicles in disease therapy. *Int J Mol Sci.* 2024;25(14):7715.
6. Khatami SH, Karami N, Taheri-Anganeh M, Taghvi S, Tondro G, et al. Exosomes: promising delivery tools for overcoming blood–brain barrier and glioblastoma therapy. *Mol Neurobiol.* 2023;60(8):4659–78.

7. Andriolo G, Provasi E, Lo Cicero V, Brambilla A, Soncin S, Torre T, et al. Exosomes from human cardiac progenitor cells for therapeutic applications: development of a GMP-Grade manufacturing method. *Front Physiol.* 2018;9:1169.
8. Zhao Y, Sun X, Cao W, Ma J, Sun L, Qian H, et al. Exosomes derived from human umbilical cord mesenchymal stem cells relieve acute myocardial ischemic injury. *Stem Cells Int.* 2015;2015:761643.
9. Yan Y, Li R, Chen H, Li Y, Wu M, Wang Z, et al. Magnetic nanoagent assisted Deciphering of heterogeneous glycans in extracellular vesicles of varied cellular origins. *Biosens Bioelectron.* 2023;241:115705.
10. Yin T, Liu Y, Ji W, Zhuang J, Chen X, Gong B, et al. Engineered mesenchymal stem cell-derived extracellular vesicles: A state-of-the-art multifunctional weapon against alzheimer’s disease. *Theranostics.* 2023;13(4):1264–85.
11. Jia H, Liu W, Zhang B, Wang J, Wu P, Tandra N, et al. HucMSC exosomes-delivered 14-3-3ζ enhanced autophagy via modulation of ATG16L in preventing cisplatin-induced acute kidney injury. *Am J Transl Res.* 2018;10(1):101–13.
12. Kim S, Lee SK, Kim H, Kim TM. Exosomes secreted from induced pluripotent stem cell-Derived mesenchymal stem cells accelerate skin cell proliferation. *Int J Mol Sci.* 2018;19(10):3119.
13. Küstermann C, Narbutė K, Movčana V, Parfejevs V, Rūmnieks F, Kaukjis P, et al. iPSC-derived lung and lung cancer organoid model to evaluate cisplatin encapsulated autologous iPSC-derived mesenchymal stromal cell-isolated extracellular vesicles. *Stem Cell Res Ther.* 2024;15(1):246.
14. Abbasi R, Nejati V, Rezaie J. Exosomes biogenesis was increased in metformin-treated human ovary cancer cells; possibly to mediate resistance. *Cancer Cell Int.* 2024;24(1):137.
15. Lisini D, Lettieri S, Nava S, Accordino G, Frigerio S, Bortolotto C, et al. Local therapies and modulation of tumor surrounding stroma in malignant pleural mesothelioma: A translational approach. *Int J Mol Sci.* 2021;22(16):9014.
16. Mirra L, Beretta GL, Lisini D, Marcianti A, Spampinato E, Corno C et al. Therapeutic strategies to improve the treatment of pleural mesothelioma. *Curr Med Chem.* 2025;32(11). <https://doi.org/10.2174/0109298673268206240405084558>
17. Silva AKA, Morille M, Piffoux M, Arumugam S, Mauduit P, Larghero J, et al. Development of extracellular vesicle-based medicinal products: A position paper of the group extracellular vesicle translation to clinical perspectiVES - EVOLVE France. *Adv Drug Deliv Rev.* 2021;179:114001.
18. Welsh JA, Goberdhan DCI, O’Driscoll L, Buzas EI, Blenkiron C, Bussolati B, et al. Minimal information for studies of extracellular vesicles (MISEV2023): from basic to advanced approaches. *J Extracell Vesicles.* 2024;13(2):e12404.
19. Malvicini R, De Lazzari G, Tolomeo AM, Santa-Cruz D, Ullah M, Cirillo C, et al. Influence of the isolation method on characteristics and functional activity of mesenchymal stromal cell-derived extracellular vesicles. *Cytotherapy.* 2024;26(2):157–70.
20. Stella G, Lisini D, Pedrazzoli P, Galli G, Bortolotto C, Melloni G, et al. Phase I clinical trial on pleural mesothelioma using neoadjuvant local administration of Paclitaxel-Loaded mesenchymal stromal cells (PACLIMES trial): Study Rationale and Design. *Cancers.* 2024;16:3391.
21. Lisini D, Nava S, Pogliani S, Avanzini MA, Lenta E, Bedini G, et al. Adipose tissue-derived mesenchymal stromal cells for clinical application: an efficient isolation approach. *Curr Res Transl Med.* 2019;67(1):20–7.
22. Lisini D, Nava S, Frigerio S, Pogliani S, Maronati G, Marcianti A, et al. Automated Large-Scale production of Paclitaxel loaded mesenchymal stromal cells for cell therapy applications. *Pharmaceutics.* 2020;12(5):411.
23. Las Heras K, Royo F, Garcia-Vallicrosa C, Igartua M, Santos-Vizcaino E, Falcon-Perez JM, et al. Extracellular vesicles from hair follicle-derived mesenchymal stromal cells: isolation, characterization and therapeutic potential for chronic wound healing. *Stem Cell Res Ther.* 2022;13(1):147.
24. Cordani N, Lisini D, Coccè V, Paglia G, Meanti R, Cerrito MG, et al. Conditioned medium of mesenchymal stromal cells loaded with Paclitaxel is effective in preclinical models of Triple-Negative breast Cancer (TNBC). *Int J Mol Sci.* 2023;24(6):5864.
25. Witwer KW, Van Balkom BWM, Bruno S, Choo A, Dominici M, Gimona M, et al. Defining mesenchymal stromal cell (MSC)-derived small extracellular vesicles for therapeutic applications. *J Extracell Vesicles.* 2019;8(1):1609206.
26. Welsh JA, Arkesteijn GJA, Bremer M, Cimorelli M, Dignat-George F, Giebel B, et al. A compendium of single extracellular vesicle flow cytometry. *J Extracell Vesicles.* 2023;12(2):e12299.
27. Takakura Y, Hanayama R, Akiyoshi K, Futaki S, Hida K, Ichiki T, et al. Quality and safety considerations for therapeutic products based on extracellular vesicles. *Pharm Res.* 2024;41(8):1573–159.

28. Adlerz K, Patel D, Rowley J, Ng K, Ahsan T. Strategies for scalable manufacturing and translation of MSC-derived extracellular vesicles. *Stem Cell Res.* 2020;48:101978.
29. Barezkai J, Refflinghaus L, Okpara M, Tasto L, Tertel T, Giebel B, et al. Process development for the production of mesenchymal stromal cell-derived extracellular vesicles in conventional 2D systems. *Cytotherapy.* 2024;26(9):999–1012.
30. Forteza-Genestra MA, Antich-Rosselló M, Ramis-Munar G, Calvo J, Gayà A, Monjo M, et al. Comparative effect of platelet- and mesenchymal stromal cell-derived extracellular vesicles on human cartilage explants using an *in vivo* inflammatory osteoarthritis model. *Bone Joint Res.* 2023;12(10):667–76.
31. Lorenzini B, Peltzer J, Goulinet S, Rival B, Lataillade JJ, Uzan G, et al. Producing vesicle-free cell culture additive for human cells extracellular vesicles manufacturing. *J Control Release.* 2023;355:501–14.
32. Almeria C, Krefß S, Weber V, Egger D, Kasper C. Heterogeneity of mesenchymal stem cell-derived extracellular vesicles is highly impacted by the tissue/cell source and culture conditions. *Cell Biosci.* 2022;12(1):51.
33. Shelke GV, Lässer C, Gho YS, Lötvall J. Importance of exosome depletion protocols to eliminate functional and RNA-containing extracellular vesicles from fetal bovine serum. *J Extracell Vesicles.* 2014; 3.
34. Kumeda N, Ogawa Y, Akimoto Y, Kawakami H, Tsujimoto M, Yanoshita R. Characterization of membrane integrity and morphological stability of human salivary exosomes. *Biol Pharm Bull.* 2017;40(8):1183–91.
35. Mentkowski KI, Snitzer JD, Rusnak S, Lang JK. Therapeutic potential of engineered extracellular vesicles. *AAPS J.* 2018;20(3):50.
36. Pieters BC, Arntz OJ, Bennink MB, Broeren MG, van Caam AP, Koenders MI, et al. Commercial cow milk contains physically stable extracellular vesicles expressing immunoregulatory TGF- β . *PLoS ONE.* 2015;10(3):e0121123.
37. Bæk R, Søndergaard EK, Varming K, Jørgensen MM. The impact of various preanalytical treatments on the phenotype of small extracellular vesicles in blood analyzed by protein microarray. *J Immunol Methods.* 2016;438:11–20.
38. Bosch S, de Beaurepaire L, Allard M, Mosser M, Heichette C, Chrétien D, et al. Trehalose prevents aggregation of exosomes and Cryodamage. *Sci Rep.* 2016;6:36162.
39. Jeyaram A, Jay SM. Preservation and storage stability of extracellular vesicles for therapeutic applications. *AAPS J.* 2017;20(1):1.
40. Yang D, Zhang W, Zhang H, Zhang F, Chen L, Ma L, et al. Progress, opportunity, and perspective on exosome isolation - efforts for efficient exosome-based theranostics. *Theranostics.* 2020;10(8):3684–707.
41. Crivelli B, Chlapanidas T, Perteghella S, Lucarelli E, Pascucci L, Brini A, et al. Italian mesenchymal stem cell group (GISM). mesenchymal stem/stromal cell extracellular vesicles: from active principle to next generation drug delivery system. *J Control Release.* 2017;262:104–17.
42. Pascucci L, Coccè V, Bonomi A, Ami D, Ceccarelli P, Ciusani E, et al. Paclitaxel is incorporated by mesenchymal stromal cells and released in exosomes that inhibit *in vitro* tumor growth: a new approach for drug delivery. *J Control Release.* 2014;192:262–70.
43. Kim MS, Haney MJ, Zhao Y, Mahajan V, Deygen I, Klyachko NL, et al. Development of exosome-encapsulated Paclitaxel to overcome MDR in cancer cells. *Nanomedicine.* 2016;12(3):655–64.
44. Saha S, Banskota S, Yousefpour P, Schaal JL, Zakharov N, Liu J, Dzuricky M, He Z, Roberts S, Li X, Chilkoti A. Preclinical development of a genetically engineered Albumin-Binding nanoparticle of Paclitaxel. *Small Sci.* 2024;4(11):2400153. <https://doi.org/10.1002/smsc.202400153>. PMID: 40213453; PMCID: PMC11934972.
45. Zhong Y, Mao Y, Fu X, Huang H. Sintilimab combined with nanoparticle Albumin-Bound Paclitaxel-Based chemotherapy in severe locally advanced or metastatic squamous NSCLC showed good efficacy and safety: A pilot retrospective analysis. *Int J Nanomed.* 2024;19:11433–44. PMID: 39534379; PMCID: PMC11555032.
46. Chen Q, Gao G, Yuan Y, Zong Y, Zhao X, Guo H. Efficacy and safety of Paclitaxel combined with oxaliplatin in the treatment of advanced primary hepatocellular carcinoma. *Am J Cancer Res.* 2025;15(3):1122–32. PMID: 40226453; PMCID: PMC11982741.
47. Rahman MA, Jalouli M, Yadab MK, Al-Zharani M. Progress in drug delivery systems based on nanoparticles for improved glioblastoma therapy: addressing challenges and investigating opportunities. *Cancers (Basel).* 2025;17(4):701. <https://doi.org/10.3390/cancers17040701>. PMID: 40002294; PMCID: PMC11852615.
48. Zarneshan SN, Aghaz F. Engineered nanoparticles as a promising drug delivery system for glioblastoma multiforme treatment. *Ther Deliv.* 2025 Mar 25:1–14. doi: 10.1080/20415990.2025.2484170. Epub ahead of print. PMID: 40134106.
49. Garofalo M, Villa A, Rizzi N, Kuryk L, Rinner B, Cerullo V, et al. Extracellular vesicles enhance the targeted delivery of immunogenic oncolytic adenovirus and Paclitaxel in immunocompetent mice. *J Control Release.* 2019;294:165–75.
50. Villa A, Crescenti D, De Mitri Z, Crippa E, Rosa S, Rizzi N, et al. Preclinical Pharmacology of patient-derived extracellular vesicles for the intraoperative imaging of tumors. *Theranostics.* 2024;14(16):6301–18.

Publisher's note

Springer Nature remains neutral with regard to jurisdictional claims in published maps and institutional affiliations.